Polym. Bull. (2017) 74:1713–1726
DOI 10.1007/s00289-016-1798-9

ORIGINAL PAPER

Improvement in toughness of polylactide/poly(butylene adipate-co-terephthalate) blend by adding nitrile rubber

Teresa Maria Dias Fernandes[1] · Márcia Christina Amorim Moreira Leite[1] · Ana Maria Furtado de Sousa[1] · Cristina Russi Guimarães Furtado[1] · Viviane Alves Escócio[2] · Ana Lucia Nazareth da Silva[2]

Received: 4 March 2016 / Revised: 29 June 2016 / Accepted: 29 August 2016 /
Published online: 6 September 2016

Abstract This paper describes the preparation and characterization of the effects of polylactide (PLA), poly(butylene adipate-co-terephthalate) (PBAT) and nitrile rubber (NBR) blends. First, a commercial PLA/PBAT blend was characterized by using the Fourier transform infrared spectroscopy and thermal gravimetric analysis. The results show that commercial blend is composed by ~70 wt% of PLA and 30 wt% of PBAT. The PLA/PBAT/NBR blends and also a reference of PLA/PBAT blend were processed by extrusion and compression molding. Then, all compositions were evaluated by their toughness and the thermal behaviors. Special attention was given to the morphology evaluated by scanning electron microscope. The result showed PLA presented in all compositions suffered thermo-mechanical degradation. However, a significant improvement in the toughness was observed for all compositions produced with NBR. That fact was proved by both Izod impact test and the morphology analyses. Additionally, the morphology comparison among the blends also shows that the addition of NBR helps to reduce the size of the PBAT domains in the PLA matrix.

Keywords Polylactide · Poly(butylene adipate-*co*-terephthalate) · Nitrile rubber · Toughness · Izod impact resistance

✉ Teresa Maria Dias Fernandes
teresamdf@hotmail.com

[1] Chemical Process Department, Rio de Janeiro State University, São Francisco Xavier, 524, Maracanã, Rio de Janeiro, RJ 20550-900, Brazil

[2] Instituto de Macromoléculas Professora Eloisa Mano, Rio de Janeiro Federal University, Av. Horácio Macedo, 2030, Centro de Tecnologia, Prédio do Bloco J, Rio de Janeiro, RJ CEP 21941-598, Brazil

Introduction

Polymers produced from petrochemical monomers have been used since the mid-twentieth century. Recognized for their outstanding properties, the polymers are used in the production of practically all necessary objects for the human life, and as a consequence, an enormous volume of polymeric waste is generated, which causes considerable environmental problems. Thus, the reduction of such negative environment impact has become a challenge that motivates both academic and industrial researchers to develop and/or improve new materials which would minimize the amount of the negative discarded of petroleum polymer based [1]. As an example, we can mention the studies regarding biopolymers, biobased plastics, bionanocomposites and biobased blends [1–3].

Nowadays, polylactide (PLA) is one of the most widely used bioplastics. It is produced preferably from ring opening polymerization of lactide monomer, which is derived from renewable resources, such as corn, sugarcane, potatoes and other sources of polysaccharides [4, 5]. Although the PLA is one of the most promising biopolymers due to its versatility, mechanical properties, optical clarity, and low cost, there are some properties, such as thermal and toughness, which still do not meet the specification requirements of many important applications, where the common petroleum-based thermoplastics are used [3]. In order to solve those drawbacks, new blends have been tested, and one of those that can be found in the market is the blending of poly(lactic acid) and poly(butylene adipate-co-terephthalate) (PBAT) [6–8], which is currently commercialized by BASF with the tradename of Ecovio®.

Poly(butylene adipate-co-terephthalate) or PBAT is a well-known biodegradable polymer in spite of being produced from petroleum-based monomers. PBAT is certified as compostable by the Biodegradable Products Institute (BPI) according to the ASTM D6400 standard [4]. PLA/PBAT blends with improved mechanical properties, particularly with a good level of toughness, have been investigated. However, since the PLA and PBAT produce an immiscible blend, those values of the toughness may not still be sufficient to meet the current specifications, principally for those blends which have high content of PLA [2, 6, 9, 10].

Some studies have been developed with the purpose of improving the PLA/PBAT toughness. The impact strength of PLA/PBAT blend at ratio of 75:25 was increased using glycidyl methacrylate as a reactive compatibilizer to improve the interface interaction between PLA and PBAT [2]. Similar toughness improvement was observed for a PLA/PBAT blend, with no less than 15 wt% of PBAT and no more than 0.5 wt% of epoxy-functional styrene acrylic copolymer, which works as a chain extender for the PLA matrix [11]. A remarkable increase of Izod impact resistance, from 28 to 110 J m^{-1}, was achieved when PLA/PBAT was in situ compatibilized using dicumyl peroxide as a free radical initiator. That in situ compatibilization led to the reduction of the PBAT domain size and enhancement the interfacial adhesion between PLA and PBAT [12].

Among the different methods used in polymer science for toughness improvement, the addition of elastomers has been the most successful technique.

Nevertheless, researches regarding rubber addition to the PLA/PBAT blend are not easily referred in the literature. It was only reported use of rubber to increase the toughness of neat PLA. As an example, two recent researches show that an improvement of ductile behavior of PLA can be obtained by adding natural rubber [13, 14]. In both researches, the authors report the lack of interfacial adhesion between the PLA and NR can be solved using epoxy-modified NR (ENR) [13] and by using peroxide-induced dynamic vulcanization [14]. Natural rubber (NR) is a polymer obtained by coagulation of latex from tree *Hevea brasilienses*. It shows high elasticity, good tensile strength and abrasion resistance. Because of its non-polar nature, it has poor interfacial adhesion to polyesters [15, 16].

Nitrile rubber (NBR) is a copolymer of acrylonitrile and butadiene monomers. Physical and chemical properties of NBR depend on the total acrylonitrile content in the rubber. The higher the nitrile content is; the higher is the oil resistance and polarity. NBR is more resistant than natural rubber to oils and acid, but it has less strength and flexibility [15, 16].

Based on what was previously exposed, the present study aims firstly at investigating the effect of the nitrile rubber (NBR) addition to a PLA/PBAT blend to improve the toughness behavior. Besides that, in order to understand how the rubber content affected the toughness on PLA/PBAT/NBR blend, we also aimed at characterizing the thermal properties and the morphology of the PLA/PBAT blends with and without rubber. Due to the fact of being a polar rubber, NBR was chosen for this study.

Materials and methods

Materials

Polylactide/poly(butilene adipate-co-terephtalate) (PLA/PBAT) blend grade ECOVIO® F2224 (MFI: 3.0–6.5 g/10 min) was supplied by BASF.

Nitrile rubber (NBR), grade NP2021, containing 33 % of acrylonitrile content and Mooney viscosity ($ML_{(1+4)}$ at 100 °C) of 47 was supplied by Nitriflex S/A Indústria e Comércio Ltda.

Blend preparation

All raw materials of each blend formulation were manually mixed and then they were dried in a forced-air oven at 60 °C for 24 h. The blends were prepared in pellet form using a Haake Thermo Scientific, model Rheomex OS PTW, co-rotating twin-screw extruder with length to diameter (L/D) ratio of 25, screw rotation of 200 rpm and output rate of 500 g h^{-1}. This extruder has five controlled temperature zones, where the following profile was set: 70/135/145/155/157/158 °C. That profile temperature was set through preliminary tests out performed with thePLA/PBAT. Figure 1 shows the screw configuration while Table 1 shows the blends formulations.

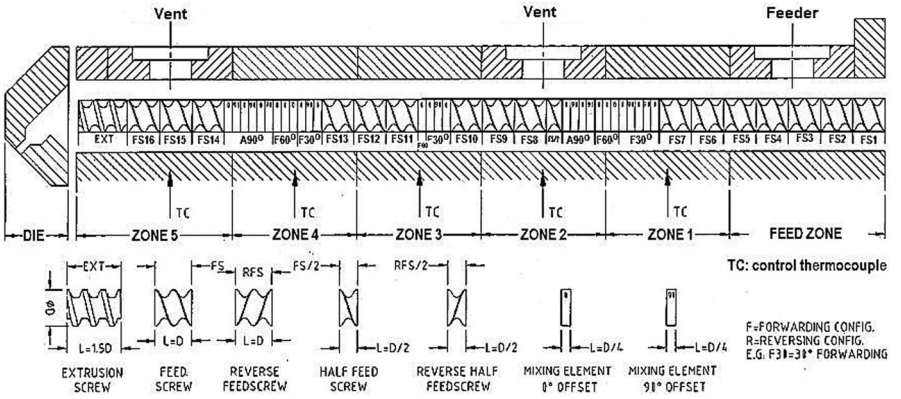

Fig. 1 Screw configuration of Haake Thermo Scientific, model Rheomex OS PTW 16

Table 1 Blend composition (wt%)

Component	B0	B10[a]	B20
Ecovio	100	90	80
NBR	0	10	20

[a] B10 was replicated twice [B10(1) and (B10(2)] so as to evaluate the process repeatability

Fourteen test specimens for each blend composition [B0, B10(1), B10(2) and B20] were prepared by compression molded by using a hydraulic press, Carver brand, model 3851-0. The mold temperature, pressure and the cooling time were set at 210 °C, 60 and 300 s, respectively. Before compression molding, all blends were dried in a forced-air oven at 60 °C for 24 h.

Characterization

Izod impact test

Izod pendulum impact resistance was performed using a CEAST Resil Impactor tester, according to ASTM D256-06a standard. That piece of equipment has an instrumented hammer, which measures the energy of both crack-initiation and crack-propagation, besides measuring the required energy to produce a total break of the test specimen. The composite results were the averaged over eight test specimens' measurements.

Thermogravimetric analysis

The thermal stability was carried out in Q500 series thermogravimetric analyzer (TA Instruments), using samples amount of $\sim$20 mg, scanning temperature from 25 to 900 °C, heating rate of 20 °C min^{-1} under nitrogen atmosphere.

Fourier transform infrared (FTIR) spectroscopy

Fourier transform infrared (FTIR) spectroscopy was performed using spectrometer (Perkin Elmer Spectrum One). Samples were analyzed using attenuated total reflectance mode (ATR) in the range of 600–4000 cm^{-1}.

Blend morphology

A JEOL JSM-6510LV scanning electron microscope (SEM) with electron beam acceleration of 20 kV in vacuum mode was used to observe the morphologies of the composites. The surfaces analyzed were from Izod impact tested and cryogenic-fractured specimens. The samples were fixed on metal support stubs using carbon tape and then coated with gold and observed with seconding electron beam detector.

Data analysis

The Izod impact data were analyzed by one-way analysis of variance (ANOVA) and least square (LS) means test by using 95 % of confidence interval. The software used was Statistica 8.

Results and discussion

PLA/PBAT commercial blend characterization by FTIR and TGA

Due to the fact that a commercial blend of PLA/PBAT was used in the study, it is mandatory to characterize the selected grade of blend (Ecovio® F2224), bearing the intention of having technical data to support the investigation.

Figure 2 shows the FTIR spectrum of a pellet of the PLA/PBAT blend, where bands, which characterized both polyester present in the blend, are observed. According to the technical literature [17, 18], bands at 1754 and 1730 cm^{-1} correspond, respectively, to the axial deformation vibration of C=O of PLA and

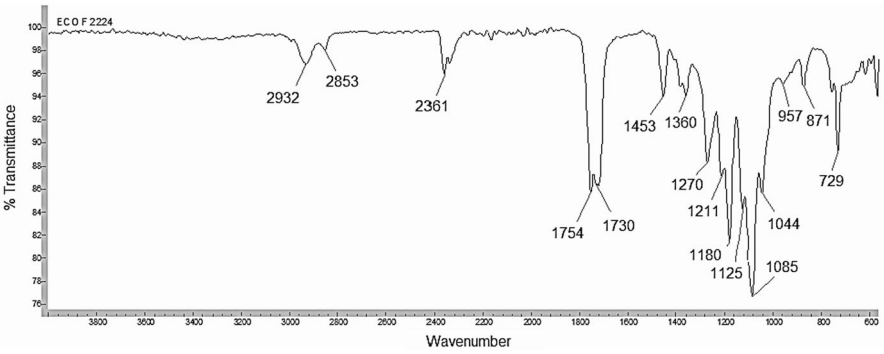

Fig. 2 PLA/PBAT commercial blend spectrum—FTIR

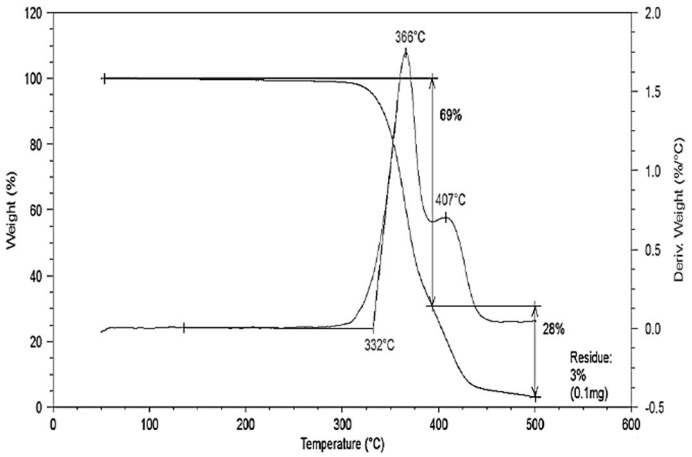

Fig. 3 TGA/DTG of PLA/PBAT commercial blend

PBAT. The presence of PLA is also confirmed by the bands at 1453 and 871 cm^{-1}, which are assigned to the –CH3 and –CH–, respectively. Regarding the PBAT, the band at 729 cm^{-1} is related to the stretch of –CH2–. Finally, the bands at 1184, 1129, 1087 and 1268 cm^{-1} correspond to the stretching of the –CO– bond, which is present in the PLA, while the same –CO– bond, which belongs to PBAT, is characterized by the presence of the 1104, 1120 and 1165 cm^{-1} bands [17, 18].

An estimation of the blend composition and thermal resistance were evaluated by TGA/DTG. According to Fig. 3, which shows the TGA/DTG curves, we noticed two degradation processes, being the first assigned to the PLA and second one to the PBAT. According to the analysis, the PLA/PBAT commercial blend is composed approximately by 70 wt% of PLA and 30 wt% of PBAT. Since the amount of PLA is higher than the PBAT content, we confirmed that PLA is the matrix while PBAT is the dispersed phase of the blend. As for the thermal resistance, the initial decomposition temperature of the blend is 332 °C, and the temperatures of maximum rate of decomposition of PLA and PBAT present in the blend are 366 and 407 °C, respectively. Those values of temperatures are in agreement with the ones reported by literature [2].

PLA/PBAT/NBR blend characterization

Thermogravimetric analysis: TGA/DTG

The thermal (TGA) and differential (DTG) thermogravimetric curves of the B0, B10(1), B10(2) and B20 blends are shown in Figs. 4 and 5, respectively. In addition, the NBR and the PLA/PBAT commercial blend (pellet) curves are also included. Table 2 shows the comparison of initial degradation temperatures ($T_{initial}$) and the temperature of the maximum rate of decomposition (T_{max}) for each degradation process.

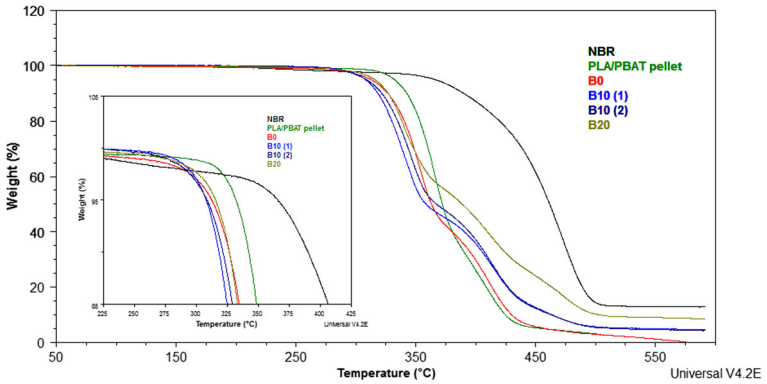

Fig. 4 TGA thermogram of B0, B10(1), B10(2), B20, NBR and PLA/PBAT (pellet)

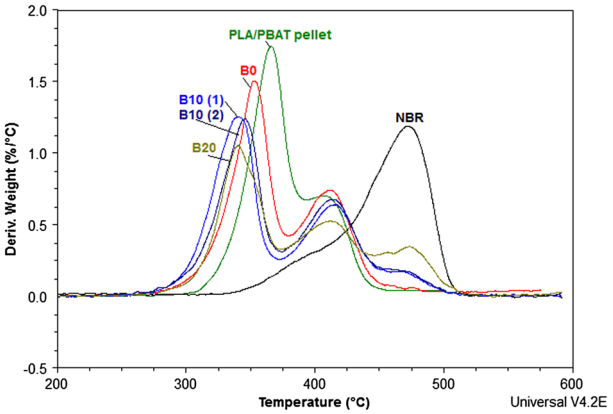

Fig. 5 DTG thermogram of B0, B10(1), B10(2), B20, NBR and PLA/PBAT (pellet)

Table 2 Thermal characterization of the PLA/PBAT/NBR, PLA/PBAT and NBR

Sample	Initial degradation temperature (T_{inital}) °C	Temperature at maximum rate of decomposition (T_{max}) °C		
		First peak	Second peak	Third peak
PLA/PBAT (pellet)	332 ± 2	366 ± 2	407 ± 2	–
NBR	408 ± 2	–	–	473 ± 2
B0	321 ± 2	353 ± 2	412 ± 2	–
B10(1)	303 ± 2	341 ± 2	415 ± 2	462 ± 2
B10(2)	306 ± 2	345 ± 2	414 ± 2	458 ± 2
B20	311 ± 2	341 ± 2	413 ± 2	473 ± 2

According to the TGA/DTG analysis, we observed two and three degradation processes for the PLA/PBAT (B0) and PLA/PBAT/NBR (B10 and B20), respectively. By comparing those degradations processes to the NBR and PLA/PBAT (pellet) ones, we can state that the first peak corresponds to degradation of PLA. The second peak is related to the degradation of the PBAT and, finally, the third peak is associated to nitrile rubber thermal degradation. Furthermore, a decrease of the initial degradation temperatures of the PLA/PBAT (B0) and PLA/PBAT/NBR (B10 and B20) is observed, which shows that all materials suffered thermo-mechanical degradations during the extrusion and mold compression processes.

By the analysis of Fig. 5, we can assert that the matrix of PLA suffered degradation process because significant reductions of T_{max} were observed in all blends. However, it is not possible to state that the same degradation occurred with the PBAT, as the NBR started to be degraded at the same temperature interval of the PBAT. Such effect might have contributed to have a non-clear visualization of the T_{max} displacement.

Cryogenic fracture surface morphology

The micrographs obtained by SEM for the cryogenic-fractured surface of the B0, B10(1), B10(2) e B20 blends are shown in Fig. 6a–d, respectively.

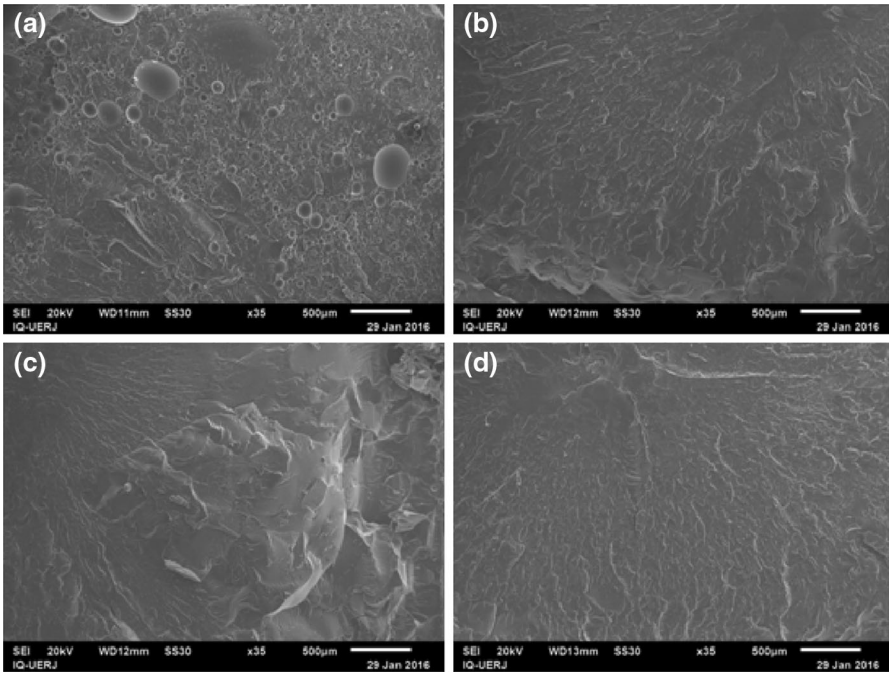

Fig. 6 Morphology SEM (35x) of the surface of the fractured by cryogenic procedure: **a** B0, **b** B10(1); **c** B10(2); **d** B20

As it can be seen in Fig. 6a, the B0 blend, composed by PLA and PBAT, is an immiscible blend which shows a clear phase separation. The PBAT domains are dispersed randomly and show a predominantly spherical shape and wide-ranging sizes. Those heterogeneous sizes of the PBAT domains suggest that during the processing of B0, the coalescence mechanism of the PBAT droplets was predominant in relation to the comminution one.

In a different way, non-dispersed phase separation is observed for the blends B10 and B20 in the magnitude of 500 μm, as shown in Fig. 6b–d. That fact suggests that, probably, the elastomer works as a compatibilizer, decreasing the interfacial tension between the PLA and PBAT and/or modifying the viscosity of the matrix. As a result, the dimension of the PBAT domains was reduced, not being visible in the magnitude used in the micrograph presented in Fig. 6 (500 μm). Those significant differences of morphology observed in the blends with and without NBR suggest that the materials may present distinct mechanical behaviors in the impact test.

Izod impact test

The Izod impact is a test that measures material resistance to impact from a swinging pendulum, and it is used to compare toughness behavior of materials. Table 3 shows the ANOVA table of fractured energy per thickness. That analysis decomposes the variance of fractured energy per thickness into two components: a between-group component and a within-group component. The *F* ratio, which in this case is equal to 118.59, is a ratio of the between-group estimate to the within-group estimate. Since the *P* value of the *F* test is less than 0.05 (*P* value is 0.0000), the hypotheses that all blends show the same fracture energy per thickness was rejected at the 95.0 % confidence level. Therefore, in order to show which blends are significantly different from each other, Fig. 7 shows the comparison of the required energy per thickness to cause a fracture in the blends. According to that comparison, there is toughness improvement of the B10 and B20 when they are compared to B0 (PLA/PBAT).

The fracture process of such material involves two steps—initiation and crack propagation. Depending on the ability of material to undergo plastic deformation before being fractured, two fracture modes can be defined, that is, ductile and brittle. While ductile materials exhibit extensive plastic deformation and high energy absorption to break, brittle materials show little or no plastic deformation and it also requires low energy for crack propagation.

Tables 4 and 5 show, respectively, the ANOVA tables of crack formation and crack propagation. In both cases, the *P* values were less than 0.05, which means that

Table 3 One-Way NOVA table of fractured energy per thickness

Source	Sum of squares	*df*	Mean square	*F* ratio	*P* value
Between groups	7408	3	2469	118.59	0.0000
Within groups	708	34	20.82		
Total	8116	37			

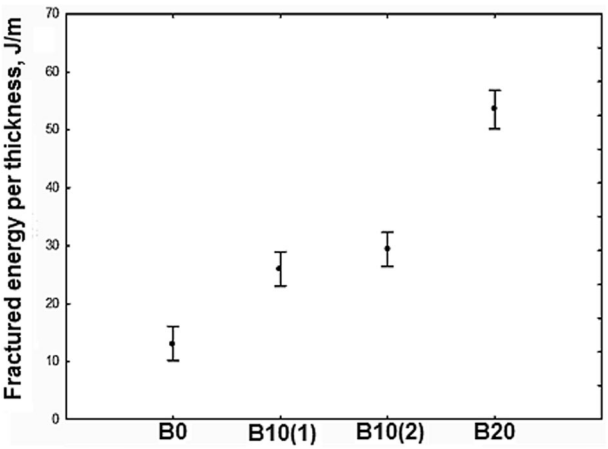

Fig. 7 Izod impact test—comparison of the fractured energy per thickness (LS means)

Table 4 One-way NOVA table of crack formation

Source	Sum of squares	*df*	Mean square	*F* ratio	*P* value
Between groups	0.0003295	3	0.0001098	8.12	0.0003
Within groups	0.00046	34	0.00001353		
Total	0.0007895	37			

Table 5 One-way NOVA table of crack propagation

Source	Sum of squares	*df*	Mean square	*F* ratio	*P* value
Between groups	0.0854	3	0.02847	105.81	0.0000
Within groups	0.009147	34	0.000269		
Total	0.09455	37			

there is a statistically significant difference between both properties from one level of blend to another at the 95.0 % confidence level.

In order to demonstrate which blends are different, Fig. 8 shows the dependence of the energy required for crack formation and crack propagation, as a function of the NBR content in the PLA/PBAT blends.

According to the Fig. 8a, the amount of energy required to initiate the crack is the same regardless of whether the content of NBR is 10 or 20 wt% However, when we compare the energy values among the blends without NBR (B0) to the ones with NBR (B10 and B20), it is possible to realize that the presence of the elastomer increased expressively the required energy to produce a crack in the material.

In contrast, as shown in Fig. 8b, the content of NBR affects the energy for crack propagation, which means that, the higher the rubber content is in the blend, the higher is the resistance of the material for crack propagation. Those results confirm that the addition of NBR improved the toughness behavior of PLA/PBAT blends.

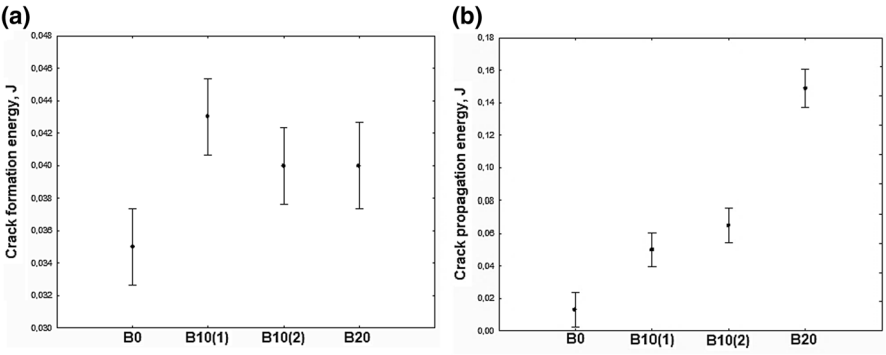

Fig. 8 Izod impact test—comparison of the crack formation (**a**) and propagation (**b**) energies

The improvement in impact strength and toughness of matrix can be explained either by the influence of rubber particles on the deformation mechanisms in the blends, or by the alteration of blend microstructure due to rubber addition. As stated in the literature [10, 19, 20], during impact fracture, the matrix will deform, and the energy will be dissipated by multiple crazing and shear yielding, being that the major occurrence of one mechanism in relation to the other is dependent on matrix nature. Since the PLA/PBAT blend shows a brittle behavior, it is expected that the failure mechanism may be predominantly composed by multiple crazing, which means that NBR rubber particles work as initiators and terminators of cracks, that is, the crack growth is interrupted and restarted when it encounters another rubber particle. However, it is known that there is not only one mechanism during fracture process, thus we expected that cavitation around the rubber particles and shear yielding also contributed to the improvement of PLA/PBAT toughness when NBR is present.

Since there is no similar research regarding adding NBR to PLA/PBAT blends, a comparison of the current results was performed with a study-related PLA/NR blend [14]. According to the authors, a super toughness improvement of the PLA by adding NR was possible due to the stretching of the rubber phase, which occurred because of the excellent interfacial adhesion between the phases. This result shows the importance that compatibility has on the blend performance. Different from NBR, NR is non-polar polymer [15, 16], which makes its mixing to a polar polymer, such as PLA, difficult. However, the increase of the compatibility between PLA and NR was only possible due to the dynamic vulcanization applied during extrusion. Authors also reported that deformation of the rubber domain was due to the extensive plastic deformation of the surrounding PLA in view of the heterogeneous stress field involved. In this current study, the vulcanization system was not used because of NBR polarity. The addition of NBR generated a toughness improvement of the blend due to its own toughness property, and also due to the change on the blend morphology with the PBAT domains size reduction. This fact suggests that NBR may have two actions: toughness and compatibilizing agents.

Blend morphology of surface from Izod impact test

The ductile and brittle behaviors can also be confirmed by the analysis of the fractured morphology of the specimens exposed to the Izod impact test. Figure 9 shows the photomicrographs of the fractured surface of the B0, B10 and B20 blends.

According to the surface morphology presented in the Fig. 9a, it is possible to verify that PLA/PBAT (B0) blend shows a smooth surface, which suggests that B0 is a brittle material. Furthermore, immiscible blend morphology is also observed, as previously reported in Sect. 3.2.2. By comparing the morphologies presented in the Fig. 6a to the Fig. 9a, we can verify that, after Izod impact test, the domains of PBAT are elongated in the direction of the crack propagation.

Regarding the PLA/PBAT/NBR blends, it is possible to verify that B10 (Fig. 9b, c) and B20 (Fig. 9d) exhibit rough morphology, which is typical for ductile materials. That rough surface is produced during the fracture process because when the generated microvoids expand, fibril bridges are formed and subsequently the coalescence of the voids occurs in order to form a crack. In addition, non-separation of phase is observed in the magnitude of the 500 μm, which confirms that NBR contributed to improve the interaction of the PLA/PBAT.

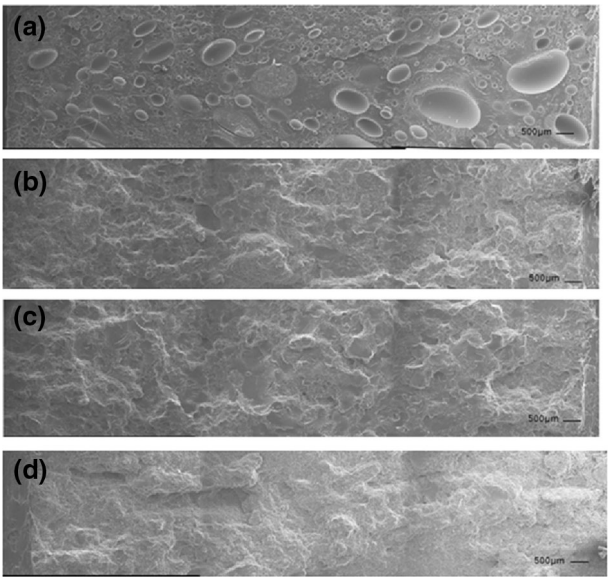

Fig. 9 Morphology SEM (35x) of the surface of the specimens from the Izod impact test: **a** B0, **b** B10(1); **c** B10(2); **d** B20

Conclusion

PLA/PBAT/NBR blends were successfully produced by extrusion and compression molding and, the addition of the elastomer has improved the toughness behavior of the PLA/PBAT blend. The results showed that NBR works as a compatibilizer, changing the blend morphology by reducing the size of the PBAT domains. From the Izod impact test, the contribution of the NBR on the energy for both initial and crack propagation was also verified. Regarding the thermal behavior, the results suggest that PLA/PBAT suffered thermo-mechanical degradation during the process.

Acknowledgments We thank Basf and Nitriflex for donating materials; LABMEV-UERJ for SEM analysis, and Fundação Carlos Chagas Filho de Amparo à Pesquisa do Estado do Rio de Janeiro—FAPERJ.

References

1. Reddy MM, Vivekanandhan S, Misra M, Bhatia SK, Mohanty AK (2013) Biobased plastics and bionanocomposites: current status and future opportunities. Prog Polym Sci 38:1653–1689. doi:10.1016/j.progpolymsci.2013.05.006
2. Kumar M, Mohanty S, Nayak SK, Parvaiz MR (2010) Effect of glycidyl methacrylate (GMA) on the thermal, mechanical and morphological property of biodegradable PLA/PBAT blend and its nanocomposites. Bioresour Technol 101:8406–8415. doi:10.1016/j.biortech.2010.05.075
3. Pivsa-Art W, Chaiyasar A, Pivsa-Art S, Yamane H, Ohara H (2013) Preparation of polymer blends between poly(lactic acid) and poly(butylene adipate-co-terephthalate) and biodegradable polymers as compatibilizers. Energy Procedia 34:549–554. doi:10.1016/j.egypro.2013.06.784
4. KijchavengkulI T, Auras R, Rubino M, Selkes S, Ngouajio M, Fernandez RT (2010) Biodegradation and hydrolysis rate of aliphatic aromatic polyester. Polym Degrad Stab 95:2641–2647. doi:10.1016/j.polymdegradstab.2010.07.018
5. Doppalapudi S, Jaina A, Khana W, Dombb AJ (2014) Biodegradable polymers—an overview. Polym Adv Technol 25:427–435. doi:10.1002/pat.3305
6. Jiang L, Wolcott MP, Zhang J (2006) Study of biodegradable polylactide/poly(butylene adipate-co-terephthalate) blends. Biomacromolecules 7(1):199–207. doi:10.1021/bm050581q
7. Dil EJ, Carreau PJ, Favis BD (2015) Morphology, miscibility and continuity development in poly(lactic acid)/poly(butylene adipate-co-terephthalate) blends. Polymer 68:202–212. doi:10.1016/j.polymer.2015.05.012
8. Gu SY, Zhang K, Ren J, Zhan H (2008) Melt rheology of polylactide/poly(butylenes adipate-co-terephthalate) blends. Carbohydr Polym 74(1):79–85. doi:10.1016/j.carbpol.2008.01.017
9. Raquez M, Nabar Y, Narayan R, Dubois P (2008) Novel high-performance talc/poly[(butylene adipate)-co-terephthalate] hybrid materials. Macromol Mat Eng 293:447–470. doi:10.1002/mame.200700352
10. Zhang L, Li C, Huang R (2005) Toughness mechanism of polypropylene/elastomer/filler composites. J Polym Sci Part B 43:1113–1123. doi:10.1002/polb.20395
11. Zhang N, Zeng C, Wang L, Ren J (2013) Preparation and properties of biodegradable poly(lactic acid)/poly(butylene adipate- co -terephthalate) blend with epoxy-functional styrene acrylic copolymer as reactive agent. J Polym Environ 21(1):286–292. doi:10.1007/s10924-012-0448-z
12. Ma P, Cai X, Zhang Y, Wang S, Dong W, Chen M, Lemstra PJ (2014) In-situ compatibilization of poly(lactic acid) and poly(butylene adipate-co-terephthalate) blends by using dicumyl peroxide as a free-radical initiator. Polym Degrad Stab 102:145–151. doi:10.1016/j.polymdegradstab.2014.01.025
13. Pongtanayut K, Thongpin C, Santawitee O (2013) The effect of rubber on morphology, thermal properties and mechanical properties of PLA/NR and PLA/ENR blends. Energy Procedia 34:888–897. doi:10.1016/j.egypro.2013.06.826

14. Yuan C, Xu C, Chen Z, Chen Y (2014) Crosslinked bicontinuous biobased polylactide/natural rubber materials: super toughness, "net-like"-structure of NR phase and excellent interfacial adhesion. Polym Test 38:78–80. doi:10.1016/j.polymertesting.2014.07.004
15. Frant I (1989) Elastomers and rubber compounding materials. Elsevier, New York
16. Mark JE, Erman B, Roland M (2013) The science and technology of rubber. Academic Press, New York
17. Al-Itry R, Lamnawar K, Maazouz A (2012) Improvement of thermal stability, rheological and mechanical properties of PLA, PBAT and their blends by reactive extrusion with functionalized epoxy. Polym Degrad Stab 97:1898–1914. doi:10.1016/j.polymdegradstab.2012.06.028
18. Sirisinha K, Somboon W (2012) Melt characteristics, mechanical, and thermal properties of blown film from modified blends of poly(butylenes adipate-co-terephthalate) and poly(lactide). J Appl Polym Sci 124:4986–4992. doi:10.1002/app.35604
19. Liang JZ, Li RKY (2000) Rubber toughening in polypropylene: a review. J Appl Polym Sci 77:409–417. doi:10.1002/(SICI)1097-4628(20000711)77:2
20. Panda BP, Mohanty S, Nayak SK (2015) Mechanism of toughening in rubber toughened polyolefin—a review. Polym Plast Technol Eng 54(5):462–473. doi:10.1080/03602559.2014.958777